

Research article

Open Access

## Crystallographic characterization of two novel crystal forms of human insulin induced by chaotropic agents and a shift in pH

Mathias Norrman<sup>1,2</sup> and Gerd Schluckebier\*<sup>1</sup>

Address: <sup>1</sup>Diabetes Protein Engineering, Novo Nordisk A/S, Novo Nordisk Park, DK-2760 Måløv, Denmark and <sup>2</sup>Molecular Biophysics, Lund University, Box 124, SE-22100 Lund, Sweden

Email: Mathias Norrman - [mtno@novonordisk.com](mailto:mtno@novonordisk.com); Gerd Schluckebier\* - [gesc@novonordisk.com](mailto:gesc@novonordisk.com)

\* Corresponding author

Published: 19 December 2007

Received: 21 August 2007

*BMC Structural Biology* 2007, **7**:83 doi:10.1186/1472-6807-7-83

Accepted: 19 December 2007

This article is available from: <http://www.biomedcentral.com/1472-6807/7/83>

© 2007 Norrman and Schluckebier; licensee BioMed Central Ltd.

This is an Open Access article distributed under the terms of the Creative Commons Attribution License (<http://creativecommons.org/licenses/by/2.0>), which permits unrestricted use, distribution, and reproduction in any medium, provided the original work is properly cited.

### Abstract

**Background:** Insulin is a therapeutic protein that is widely used for the treatment of diabetes. Its biological function was discovered more than 80 years ago and it has since then been characterized extensively. Crystallization of the insulin molecule has always been a key activity since the protein is often administered by subcutaneous injections of crystalline insulin formulations. Over the years, insulin has been crystallized and characterized in a number of crystal systems.

**Results:** Interestingly, we have now discovered two new crystal forms of human insulin. The crystals were obtained when the two chaotropic agents, urea and thiocyanate were present in the crystallization experiments, and their structures were determined by X-ray crystallography. The crystals belong to the orthorhombic and monoclinic crystal systems, with space groups  $C222_1$  and  $C2$  respectively. The orthorhombic crystals were obtained at pH 6.5 and contained three insulin hexamers in  $R_6$  conformation in the asymmetric unit whilst the monoclinic  $C2$  crystals were obtained at pH 7.0 and contained one  $R_6$  hexamer in the asymmetric unit. Common for the two new crystals is a hexamer-hexamer interaction that has not been found in any of the previous crystal forms of insulin. The contacts involve a tight glutamate-glutamate interaction with a distance of 2.3 Å between groups. The short distance suggests a low barrier hydrogen bond. In addition, two tyrosine-tyrosine interactions occupying a known phenol binding pocket contribute to the stabilization of the contacts. Within the crystals, distinct binding sites for urea were found, adding further to the discussion on the role of urea in protein denaturation.

**Conclusion:** The change in space group from  $C222_1$  to  $C2$  was primarily caused by an increase in pH. The fewer number of hexamer-hexamer interactions comprising the short hydrogen bond in the  $C2$  space group suggest that pH is the driving force. In addition, the distance between the two glutamates increases from 2.32 Å in the  $C222_1$  crystals to 2.4 Å in the  $C2$  crystals. However, in both cases the low barrier hydrogen bond and the tyrosine-tyrosine interaction should contribute to the stability of the crystals which is crucial when used in pharmaceutical formulations.

### Background

The therapeutic hormone insulin is a small protein used daily in the medical treatment of diabetes by millions of

people. The primary administration route is by subcutaneous injections of microcrystals or mixtures of microcrystals and amorphous protein. After subcutaneous

injection, the insulin crystals dissolve slowly, thus leading to a slow intermediate release of insulin into the blood stream. Ever since the biological function of insulin was discovered in the 1920s [1], the molecule has been widely characterized both biophysically and structurally. The crystallographic structure was one of the first protein structures determined [2]. It has since then been crystallized in a number of space groups of which the most common belong to the monoclinic, rhombohedral, cubic and tetragonal crystal forms. The type, size and morphology of the crystals affect how fast insulin is released, which is why crystallization of insulin has been studied extensively. Alternative administration routes are presently a rapidly expanding research field and insulin microcrystals may be well suited for other delivery methods, including pulmonary delivery or sustained release formulations [3-5]. The insulin molecule consists of two chains, A and B, with 21 and 30 residues respectively. Chain A is built up by two helical fragments separated by a short loop linked to one of the helices by an intra-chain disulfide bond. Two additional disulfide bonds link chain A to the larger chain B. In the biologically active form, insulin exists as a monomer in which chain B contains a central helical region flanked by two elongated parts. In the presence of divalent ions like zinc, the monomers assemble into hexamers [6], where each of the two central zinc ions is coordinated by three histidine residues. In the hexameric form, chain B has been shown to exist in two allosteric states denoted T and R [7]. The R state has two allosteric binding sites usually referred to as the phenolic binding site and HisB10 anion site. The T → R state transition and the two different B chain conformations, referred to as T<sub>6</sub> and R<sub>6</sub>, have been described by spectroscopic and crystallographic studies. The T<sub>6</sub> conformation, which is characterized by an extended conformation of residues 1–8 of chain B, is obtained at low chloride concentrations and in absence of phenol derivatives [8,9]. Phenolic derivatives are used as preservative in insulin pharmaceutical formulations. The most commonly used are phenol, meta-cresol, resorcinol and methylparaben. The R conformation is obtained in presence of these derivatives and at high chloride concentrations. In this form the first eight residues of the B chain adopt a helical conformation, which together with the central helical segment gives a continuous helix which includes residues B1 to B19 [10-13]. This transition from an extended to an alpha-helical conformation causes the first residue of chain B, PheB1 to undergo a ~30 Å shift in position. Although chloride is the most commonly used anion, other anions such as SCN<sup>-</sup>, OCN<sup>-</sup>, CN<sup>-</sup>, N<sub>3</sub><sup>-</sup> and NO<sub>2</sub><sup>-</sup> have also been shown to be useful [7,14,15]. Like chloride, in the absence of phenolic derivatives and at high concentrations, these anions are able to induce the R state in three of six monomers in a hexamer. The remaining three monomers have an extended conformation (T state) in the region including residues B1 to B8. The R

state of the first three monomers is incomplete with residues B4 to B8 in a helical conformation, while residues B1 to B3 have an extended conformation. This hexamer configuration is denoted T<sub>3</sub>R<sub>3</sub><sup>f</sup>, where the 'f' indicates a frayed R conformation [16,17].

We here present a study which shows that certain chaotropic additives can induce two novel types of insulin crystals, and that the type of crystals formed depends on the charge state of insulin, i.e. is pH dependent. The structures and crystal packing interaction of the two new crystal forms have been analyzed and compared to crystal packing interactions in other previously known insulin crystals.

## Results and discussion

Crystallization of insulin is of high importance in pharmaceutical formulations and in insulin manufacturing and has been systematically investigated since the 1920s [6,18-20]. By introducing chaotropic agents in the crystallization experiments, we succeeded in identifying two new crystal forms of native human insulin. The crystals were found using two different crystallization experiments. The first crystals were obtained in a crystallization screen with varying concentrations of urea and sodium chloride in presence of zinc and resorcinol. The crystals were initially characterized by X-ray powder diffraction and were shown to have a powder pattern differing from previously known insulin crystal forms [21]. Further optimizations of crystallization conditions resulted in crystals suitable for single crystal analysis and determination of crystal system which was found to be orthorhombic in space group C222<sub>1</sub>. The crystals appeared in the pH range 6.0 – 6.5 while a second type of crystals, characterized as monoclinic with space group C2 grew in the pH range 6.5 – 7.0. In the overlapping pH interval around pH 6.5, the C222<sub>1</sub> crystals were present in wells with lower salt and urea concentrations. A few drops contained a mixture of the two crystal types. In a parallel experiment, the urea and sodium chloride were substituted for thiocyanate. Interestingly, the same two crystal types appeared here, at the same pH intervals, with a clearer pH distinction at pH 7.0. Crystallization with thiocyanate or chloride ions without a phenol derivative has previously been shown to stabilize the T<sub>3</sub>R<sub>3</sub><sup>f</sup> form of hexameric insulin in a rhombohedral crystal system [16,17]. In our case when resorcinol and thiocyanate were present, the orthorhombic C222<sub>1</sub> and monoclinic C2 crystals appeared. The well characterized monoclinic crystals in space group P2<sub>1</sub> [10,11] were present at pH values above 7.0 in wells with low salt and high urea concentration and increased in frequency as the pH was raised to become the dominating crystal form at pH ≥ 7.5. The crystals obtained in presence of urea will be referred to as C222<sub>1</sub>urea and C2urea while the two crystal

forms obtained with thiocyanate are referred to as C222<sub>1</sub>scn and C2scn.

#### Structure of insulin in the orthorhombic lattice

The crystals grown at pH 6.5, from both the urea- and thiocyanate (NaSCN) screen, were found to belong to space group C222<sub>1</sub> with unit cell parameters  $a = 59 \text{ \AA}$ ,  $b = 220 \text{ \AA}$ ,  $c = 223 \text{ \AA}$ . The asymmetric unit contains three insulin hexamers with a crystal solvent content of 64%. The hexamers have R<sub>6</sub> conformation and contain two zinc atoms/hexamer coordinated to three histidine residues (HisB10). In the C222<sub>1</sub>urea crystal, the zinc is additionally coordinated by a chloride ion at an average distance of  $2.15 \pm 0.10 \text{ \AA}$ , whilst in the C222<sub>1</sub>scn crystal structure the chloride ion is replaced by a thiocyanate. The thiocyanate coordinates to zinc through its nitrogen atom with an average distance of  $1.82 \pm 0.04 \text{ \AA}$ . The three hexamers in the asymmetric unit are arranged in an angular formation where the central hexamer connects the two outer hexamers with an angle of  $\sim 110^\circ$ , Figure 1a. The non-crystallographic three-fold axes which pass through the two zinc atoms in each hexamer are almost orthogonal to each other. In both the C222<sub>1</sub>urea and C222<sub>1</sub>scn structures, one co-crystallized resorcinol molecule is bound to each insulin monomer in the phenolic binding pocket. The resorcinol molecule is hydrogen bonded with its first hydroxy group to the carbonyl O atom of CysA6 (average distance  $2.6 \text{ \AA}$ ), and the N atom of CysA11 (average distance  $2.9 \text{ \AA}$ ). The second hydroxy group hydrogen bonds to a water molecule with an average distance of  $2.7 \text{ \AA}$ . This water molecule forms another hydrogen bond to the O atom of CysA11 with an average distance of  $2.8 \text{ \AA}$ . In the final stages of refinement, one glycerol molecule was modeled into the C222<sub>1</sub>scn structure at a position where it interacted through its oxygen atoms with the amide nitrogen of PheB1 ( $2.9 \text{ \AA}$ ) and the carbonyl oxygen of ThrA8 ( $2.9 \text{ \AA}$ ). The crystal packing of the C222<sub>1</sub>urea structure is shown in Figure 1b.

#### Structure of insulin in the monoclinic lattice

The crystals obtained at slightly higher pH (pH 7.0) belong to the monoclinic space group C2 with cell dimensions  $a = 100 \text{ \AA}$ ,  $b = 60 \text{ \AA}$ ,  $c = 62 \text{ \AA}$ ,  $\beta = 116^\circ$ . They contain one hexamer with R<sub>6</sub> conformation in the asymmetric unit and have a solvent content of 50%. The crystal packing is shown in Figure 1c. Both the C2urea and C2scn structures have two zinc atoms/hexamer located  $14.7 \text{ \AA}$  and  $15.2 \text{ \AA}$  apart respectively. The zinc coordination is identical to the C222<sub>1</sub> crystals. In the C2urea structure, two additional resorcinol molecules could be fitted into the electron density. The location of the first is very close to binding site II, described in [13]. At this site, the first hydroxy group of the resorcinol molecule is hydrogen bonded to the OG atom of SerB9 ( $2.9 \text{ \AA}$ ) in an alternating conformation. The other hydroxyl group interacts with the carbonyl oxygen of GluB13 ( $2.5 \text{ \AA}$ ) and a water mole-

cule ( $3.1 \text{ \AA}$ ). The water molecule, in turn, makes a hydrogen bond to the carbonyl oxygen of SerB9 ( $3.1 \text{ \AA}$ ). In contrast to the phenolic binding interactions observed earlier in the PDB entry 1ZEG[13], where the phenolic oxygen hydrogen binds to HisB5, the angular orientation of the HisB5 in the C2urea structure does not seem to permit any interaction with the resorcinol molecule. The second additional resorcinol is located at the surface of the insulin in a solvent channel between two monomers, surrounded by water molecules. At the end of refinement, one glycerol molecule from the cryo-solution was added to both C2 structures. The glycerol molecule in the C2scn structure was found at a corresponding position as in the C222<sub>1</sub>scn structure, while the glycerol molecule in the C2urea structure was found in the solvent channel leading towards one of the zinc atoms, where it interacted with surrounding water molecules.

Refinement statistics for the four crystal forms is shown in Table 1. 95.4% of the residues in the C222<sub>1</sub>urea structure were found in the most favored regions of the Ramachandran plot and 4.6% in additional allowed regions. For the C222<sub>1</sub>scn structure, the corresponding values were 95.8% and 4.2% and for the C2 structures (C2urea/C2scn) 96.4%/96.0% and 3.6%/4.0%, respectively. The models showed no residues located in the generously allowed or disallowed regions of the plot.

All four insulin molecules are structurally very similar. Pair-wise superposition and comparison of the C2 structures results in a root-mean-square (r.m.s.) distance between corresponding C<sub>α</sub> atoms of  $0.35 \text{ \AA}$  and of  $0.88 \text{ \AA}$  when all common atoms are included. For the C222<sub>1</sub> structures the same r.m.s. distances are  $0.26 \text{ \AA}$  and  $0.58 \text{ \AA}$ .

A common feature of the four structures is the disruption of the otherwise characteristic continuous  $\alpha$ -helix from residue B1 to B19. Instead of having  $\alpha$ -helical conformation, some of the PheB1 residues in all four structures have a non-helical conformation. In the C222<sub>1</sub> structures, the majority of the B-chains (11/18 and 14/18 in the C222<sub>1</sub>urea and C222<sub>1</sub>scn structures respectively) have this conformation (conformation I) where the  $\phi/\psi$  values of ValB2 are  $-80/+45$ . In the second conformation (II), the  $\phi/\psi$  values are  $\sim -60/-45$ , closer to the typical values for an  $\alpha$ -helix. The different B-chain conformations are illustrated in Figure 2, where they are superposed on each other. The distance between the C<sub>α</sub>-atom of the PheB1 residue in the two different conformations is  $\sim 6 \text{ \AA}$ . For some of the residues, electron density could be seen for backbone atoms in more than one orientation. In such cases, the conformation with highest density was chosen, where also side chain atoms could be modeled with confidence. It should be noted that the density is weak for the side chain atoms of the Phe1 residue in chains B, F, b, f, h, j

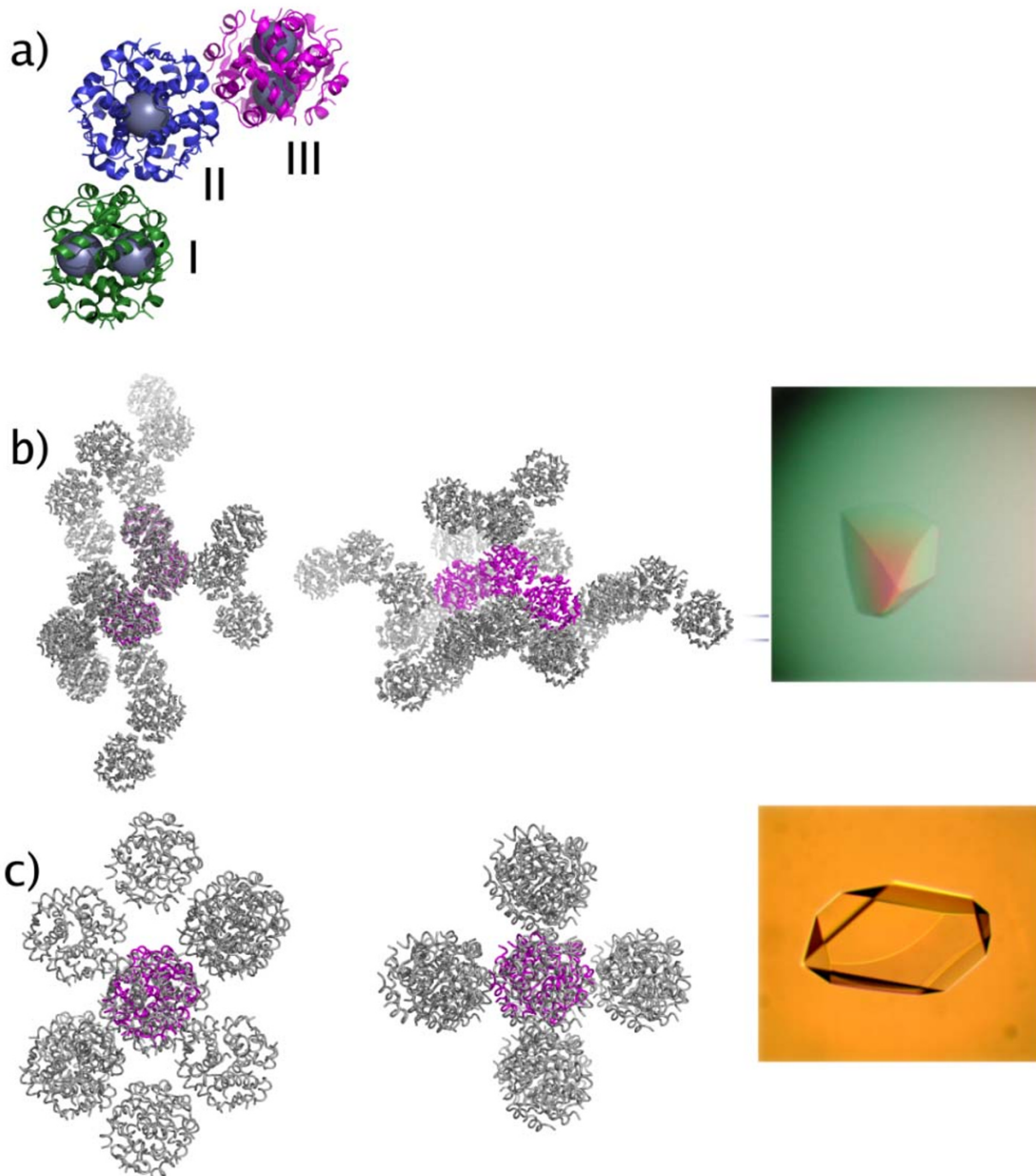


**Figure 1**

**Crystal packing.** (a) The asymmetric unit of the C222<sub>1</sub> crystal form viewed down the non-crystallographic three-fold axis of the central hexamer. The flanking hexamers are located around the central hexamer at an angle of ~110°. The local non-crystallographic three-fold axis of the two outer hexamers is almost orthogonal to the central non-crystallographic three-fold axis. The zinc atoms are illustrated as large spheres to mark the position of the three-fold axes. The hexamers are numbered from I to III. (b) The crystal packing in the C222<sub>1</sub> space group drawn with main chain trace with the asymmetric unit in magenta. (c) The crystal packing of the human insulin in space group C2. The asymmetric unit molecule is colored magenta. The inserts in (b) and (c) show crystals of the C222<sub>1</sub> and C2 forms, respectively.

**Table 1: Data processing and refinement statistics for the orthorhombic and monoclinic insulin crystallized in presence of urea and thiocyanate respectively.**

	Data sets		Na-SCN containing crystals	
	Urea containing crystals C222 <sub>1</sub> urea	C2urea	C222 <sub>1</sub> scn	C2scn
<i>Data processing</i>				
Values in parenthesis are for the highest resolution shell				
Wavelength (Å)	1.0	1.1	1.3	1.3
Cell axis a, b, c (Å)	58.9, 219.3, 223.7	100.2, 60.2, 62.9	59.0, 219.5, 224.5	100.6, 60.8, 62.1
Cell angles α β γ (deg)	90.0 90.0 90.0	90.0 116.2 90.0	90.0 90.0 90.0	90.0 116.1 90.0
Temperature (K)	100	100	100	100
Diffraction limit (Å)	2.05	1.70	1.97	1.70
Highest resolution shell (Å)	2.1 – 2.05	1.75 – 1.70	2.0 – 1.97	1.75 – 1.704
No. of observations	450 276 (23593)	72 333 (3616)	885 954 (9682)	143 773 (4037)
Unique reflections	91 251 (6331)	34 195 (1952)	102 732 (3997)	34 924 (1890)
Redundancy	4.9 (3.7)	2.1 (1.8)	8.6 (2.4)	4.1 (2.1)
R <sub>merge</sub> <sup>a</sup> (%)	8.6 (39.3)	3.4 (16.9)	9.0 (37.3)	4.3 (13.3)
I/σ (I)	11.6 (3.2)	13.7 (4.1)	17.7 (2.4)	21.6 (6.5)
<i>Refinement statistics</i>				
Values in parenthesis are for the highest resolution shell				
Resolution range (Å)	28.31 – 2.05	19.57 – 1.70	19.99 – 1.97	19.78 – 1.70
Highest resolution shell (Å)	2.10 – 2.05	1.74 – 1.70	2.02 – 1.97	1.75 – 1.704
No. of reflections	86 749 (6376)	32 471 (1621)	97 508 (6629)	33 178 (1700)
Completeness	99.9 (100)	92.3 (62.5)	99.5 (93.1)	94.8 (67.5)
R value (%) <sup>b</sup>	18.4 (21.3)	18.5 (22.9)	17.5 (21.7)	17.8 (25.5)
R <sub>free</sub> value (%) <sup>b</sup>	22.7 (28.8)	22.3 (33.4)	21.1 (25.4)	22.1 (33.1)
r.m.s.d. <sup>c</sup>				
Bond length (Å)	0.016	0.012	0.014	0.011
Bond angles (deg)	1.6	1.3	1.4	1.3
B factors (Å <sup>2</sup> ) <sup>d</sup>				
Average all atoms	32.2	27.2	33.8	20.9
All PheB1	40.1 (18)	27.4 (6)	42.4 (18)	18.7 (6)
α-helical PheB1	42.0 (7)	29.5 (3)	36.8 (5)	21.7 (3)
Non-helical PheB1	38.9 (11)	25.4 (3)	43.6 (13)	15.8 (3)

<sup>a</sup> R<sub>merge</sub> = Σ|I<sub>i</sub> - I|/ΣI where I<sub>i</sub> is an individual intensity measurement and I is the mean intensity for this reflection.

<sup>b</sup> R value = crystallographic R-factor = Σ|F<sub>obs</sub> - F<sub>calc</sub>|/Σ|F<sub>obs</sub>|, where F<sub>obs</sub> and F<sub>calc</sub> are the observed and calculated structure factors respectively.

R<sub>free</sub> value is the same as R value but calculated on 5% of the data not included in the refinement.

<sup>c</sup> Root-mean-square deviations of the parameters from their ideal values.

<sup>d</sup> Figures in parenthesis indicate number of monomers in each group.

and I in the C222<sub>1</sub>scn structure and chains h, j, l in the C222<sub>1</sub>urea structure (chain names refer to the continuous naming convention of all chains in the PDB file). The PheB1 orientations in the C2 structures resemble those of the C222<sub>1</sub> structures. Three out of the six B-chains in each structure have a non-helical conformation. The electron density is generally better defined in these two structures, which is reflected in the crystallographic B-factors. A comparison of the B-factors shows that PheB1 residues with non-helical conformation have a lower B-factor in three of the four structures, Table 1.

In contrast to the T<sub>3</sub>R<sub>3</sub><sup>f</sup> conformation, where B1–B3 have an extended conformation, only residues B1–B2 have a non-helical state. A similar, non-helical conformation of

the PheB1 residue has previously been observed for one of the B-chains in an R<sub>6</sub> insulin in complex with resorcinol (PDB ID: 1EVR) [11]. In that case, the carbonyl oxygen of PheB1 is coordinating a sodium ion which was further coordinated by the C terminal AsnA21 of a symmetry-related molecule. In our case, PheB1 is stabilized in a non-helical conformation by a hydrogen bond between amide nitrogen of PheB1 to the carbonyl oxygen of ThrA8 in a neighboring molecule, or a hydrogen bond between the carbonyl oxygen of PheB1 and the amide nitrogen of AsnB3 in the same chain. There are further interactions with symmetry-related molecules, such as the PheB1 amide nitrogen interactions with the OH group of a symmetry-related TyrA14, or the carbonyl oxygen of CysA20 and AsnA18.

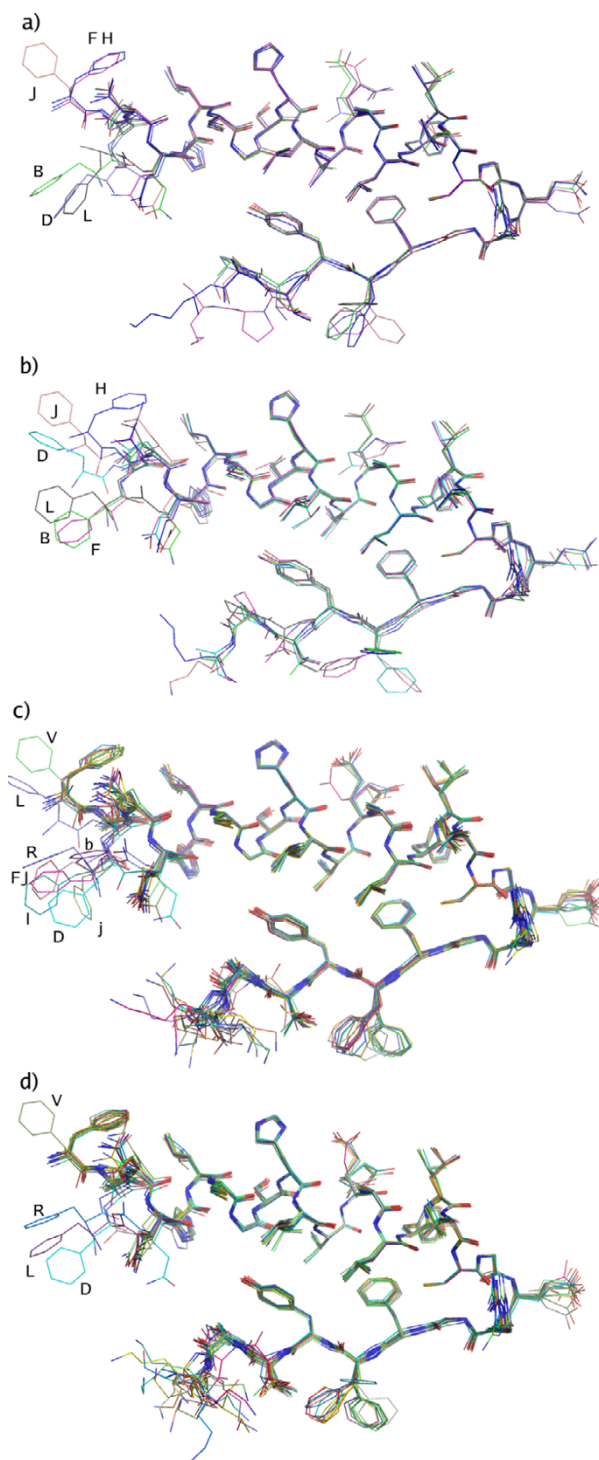


### Figure 2

**Superposed B chains from the four structures.** (a) C2urea, (b) C2scn, (c) C222<sub>1</sub>urea and (d) C222<sub>1</sub>scn. Three B chains in each of the two C2 structures and the majority of the B chains in the C222<sub>1</sub> structures have the PheB1 residue in an extended conformation (the top most population). Labels indicate chain names used in the final PDB files. For illustrative purpose, the side chain of the C-terminal LysB29 is included in the figures to illustrate the flexibility. This side-chain was subsequently omitted from several chains in the final PDB files due to disordered electron density.

In close proximity to the PheB1 residue of the three B chains with non-helical conformation in the C2urea structure there was an electron density peak with a height of  $5\sigma$  in the  $2F_o - F_c$  map and  $\sim 5\sigma$  in a  $F_o - F_c$  difference map. The location of the peak was close to the position where the carbonyl oxygen of PheB1 would be located if the conformation was  $\alpha$ -helical. Given the observed electron density, a chloride ion was fitted into this position. It is coordinated to the amide nitrogen of HisB5 ( $3.2\text{ \AA}$ ) and two or three water molecules at an average distance of  $3.3\text{ \AA}$ . The corresponding sites in the C222<sub>1</sub>urea structure were too disordered to be interpreted in a similar manner.

Location of main-chain and side-chain atoms was ambiguous for the residues LysB29 and ThrB30 in most of the chains in the four structures. Furthermore, the following residues were modeled with alternating side chain conformations; C2urea structure: GlnB4.2, SerB9.5, ValB18.5, LeuB17.6; C2scn structure: GluB13.3, ValB18.4; C222<sub>1</sub>urea structure: LeuB17.I.1, ArgB22.I.4, GlnB4.I.6, ValB18.II.4, AsnB3.III.1; C222<sub>1</sub>scn structure: ValB18.I.2, ValB18.II.4, ValB18.II.5 (the roman numerals refer to the hexamer number while the single integer following a punctuation indicates monomer).

#### Crystal packing

There is a strikingly high similarity between the crystallographic contact surfaces of the C222<sub>1</sub> and C2 crystal

forms. For five of the six contact sites found in the C2 crystal form, there is a corresponding contact surface with equivalent residue composition in the C222<sub>1</sub> structure. Each hexamer in the C222<sub>1</sub> structure has one symmetry-related contact surface that is identical to the hexamer-hexamer contact in the asymmetric unit. Including the hexamer-hexamer contacts within the asymmetric unit results in five such contact interfaces. In comparison, the C2 structure has in total six neighboring symmetry-related hexamers of which only one has the same kind of pairwise interactions as the asymmetric hexamer-hexamer contact in the C222<sub>1</sub> structure. An overview of the crystal contacts in the C222<sub>1</sub> and C2 crystals is shown in Figure 3.

#### A special crystal interaction at the dimer-dimer interface

Each of the two hexamer-hexamer interfaces in the asymmetric unit of the C222<sub>1</sub> crystals involves tyrosine-tyrosine interactions between different Tyr A14 groups. Tyr A14 is located at the dimer-dimer interface within the insulin hexamer so that the crystal packing brings four different Tyr A14 groups in proximity, Figure 4. The tyrosine side chains are pair wise stacked, such that the OH-group of TyrA14 in the first hexamer hydrogen bonds to the backbone oxygen of a TyrA14 in the neighboring hexamer ( $2.8\text{ \AA}$ ). The OH-group of the latter TyrA14 forms, in turn, hydrogen bonds to two water molecules. The polar interactions between the hexamers, Figure 4, comprise hydrogen bonds between GlnA15.I NE2 – GluA17.II OE2 ( $3.0$

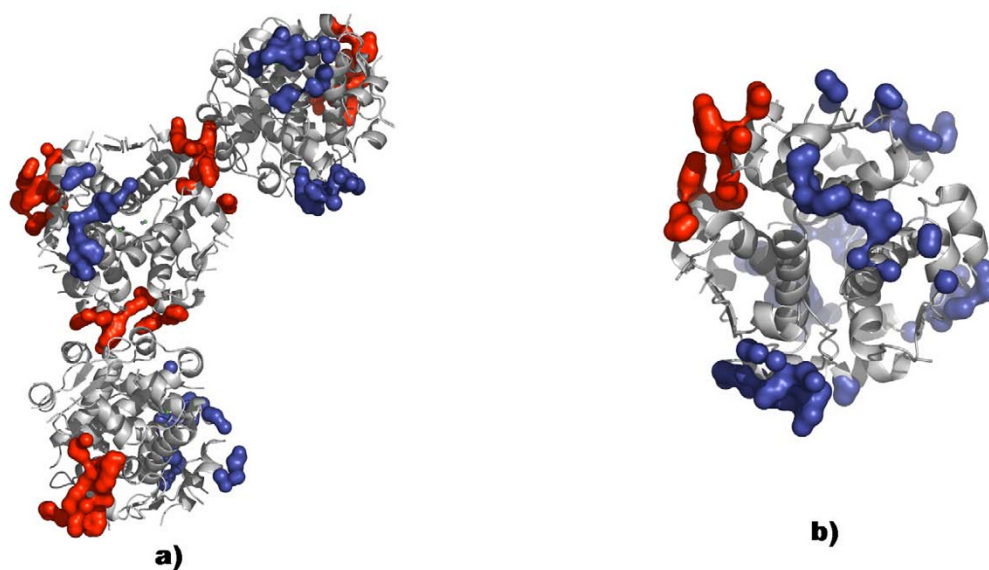


**Figure 3**

**Overview of the crystal contacts.** The crystal contacts in the C222<sub>1</sub> (a) and C2 (b) crystals are shown in sphere representation where the interfaces comprising the tyrosine-tyrosine and glutamate-glutamate interaction are shown in red.

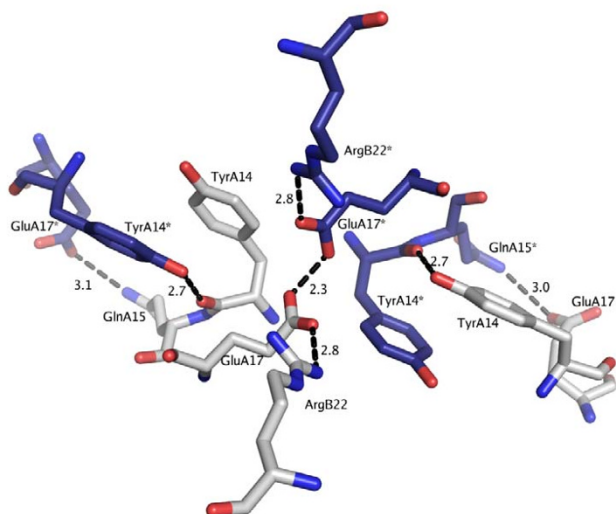


**Figure 4**  
**One of the hexamer-hexamer interfaces in the C222<sub>1</sub> urea structure.** The two tyrosine-tyrosine interactions (TyrA14-TyrA14\*) are flanking a close glutamate-glutamate contact of 2.3 Å. Both glutamates interact with ArgB22 (distance 2.8 Å). There are further two contacts between a GluA17 and GlnA15 from the neighboring hexamer. Residues from the neighboring hexamer are colored blue and marked with an \*. Distances are given in Ångström (Å).

Å), GluA17.I OE1 - GlnA15.II NE2 (3.1 Å) (.I or .II denotes different hexamers). Additionally, there is an unusually short contact between two glutamates, GluA17.I OE1 - GluA17.II OE1 (2.32 ± 0.07 Å). In spite

of the relative high pH of 6.5, the short Glu-Glu distance suggests a protonated carboxyl group of one of the glutamates. Normally, the pK<sub>a</sub> value for an exposed glutamate residue is ~4.4 in water environment. Given that GluA17 is protonated, the pK<sub>a</sub> value must thus be higher. One arginine (ArgB22) is located 2.8 Å from each glutamate and could potentially shift the pK<sub>a</sub> value by its inductive effect. The pK<sub>a</sub> value could also be shifted by the surrounding hydrophobic environment. GluA17 is flanked by the two tyrosine-tyrosine interactions, and it is conceivable that an uncharged protonated glutamate is more favorable in that environment. The short distance is indicative of a strong, low barrier hydrogen bond, where the proton is shared between the two carboxylates. Such low barrier hydrogen bonds have been found in protein active sites as part of enzyme catalysis [22,23] but also on protein surfaces [24].

As the pH is increased to 7.0, the second crystal form C2 appears. In this crystal form, there is only one crystal packing interaction comprising the tight glutamate-glutamate and tyrosine-tyrosine interaction, Figure 3. The increased pH could be the reason for the smaller number of such contacts. At higher pH, the shared hydrogen between the two glutamates becomes more delocalized and the repulsive forces will dominate. Consequently, the distance between the carboxylates is longer, 2.40 Å, versus 2.32 Å for the C222<sub>1</sub> structures, indicating a weaker interaction at this pH. At pH values above 7.5, only the monoclinic P2<sub>1</sub> crystal form [11] is observed, in which no such interface exists.

Interestingly, the position occupied by the tyrosine from a neighboring hexamer is known to bind phenolic compounds like resorcinol and m-cresol [11,13]. In Figure 5a-c the phenolic binding sites in the pdb files 1EVR (R<sub>6</sub> hex-

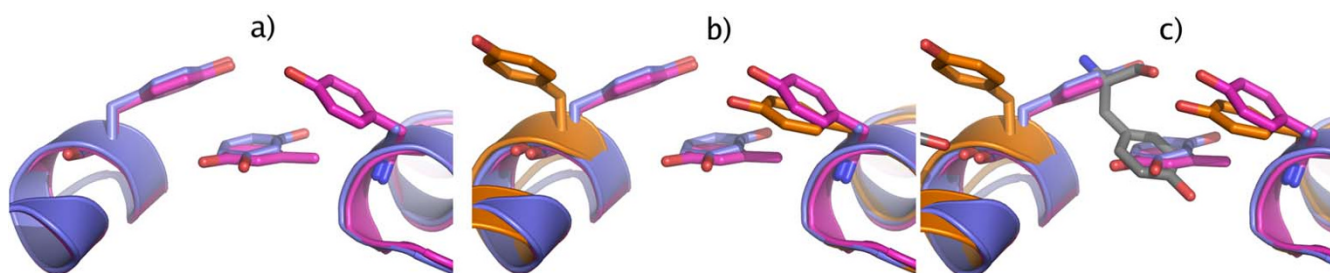


**Figure 5**  
**Comparison of the binding pocket for a phenol derivative as seen in other structures and the position for hexamer-hexamer interaction as observed in this study.** In (a), the phenolic binding pockets of 1EVR (blue) and 1EV6 (purple) are superposed. One resorcinol and one meta-cresol molecule is shown to bind in the pocket created by the two flanking tyrosine residues. The side chain of the tyrosine to the right in 1EVR is missing in the pdb file. In (b) the same structures are superposed with the C222<sub>1</sub> urea structure (orange). The side chain of the left tyrosine is flipped to accommodate the hexamer-hexamer interaction shown in (c), where a neighboring hexamer from the asymmetric unit is included (grey). The tyrosine side chain of the second hexamer occupies the same position as the phenolic compounds.



americ insulin complexed with resorcinol) and 1EV6 ( $R_6$  hexameric insulin complexed with m-cresol) [11] are compared with one of the hexamer-hexamer interfaces in the C222<sub>1</sub>urea structure. The phenyl ring of the neighboring tyrosine superposes the phenolic derivatives and should contribute to the stability of both the hexamer contact and the insulin structure.

### Analysis of crystal contact surfaces

In order to compare the different crystal forms of insulin, the contact sites were characterized by means of polarity and contact area. A summary of the properties for the various contact sites for the four structures presented in this study is shown in Table 2. Data for other crystal forms of hexameric insulin are also included. The surface area buried by crystal contacts range from 1423 Å<sup>2</sup> to 3314 Å<sup>2</sup>, which constitutes a fraction of buried surface area of between 10.6% and 24%. The smallest value is found for the orthorhombic C222<sub>1</sub> crystals where the total contacts surface for the three hexamers is 4269 Å<sup>2</sup>, which amounts to a contact surface of 1423 Å<sup>2</sup>/hexamer. The largest surface area originates from the rhombohedral crystal form, space group R3 with T<sub>6</sub> configuration of the B-chain, PDB ID: 1MSO [9]. The monoclinic crystals in space group C2 and P2<sub>1</sub> as well as the tetragonal crystal in space group P4<sub>3</sub>2<sub>1</sub>2 all have six contact sites while the rest have eight.

The size of individual contact sites ranges from 236 Å<sup>2</sup> to 414 Å<sup>2</sup>.

The contact surfaces were characterized as either polar (oxygen and nitrogen atoms, including ionisable groups) or non-polar (carbons). The four structures presented in this study constitute a group with a high fraction of non-polar contact surface, ranging from 53% to 56% of the total contact area, compared to 41% to 50% for the other crystal forms. The monoclinic P2<sub>1</sub> crystal form is the most hydrophilic, with a 40/60 distribution between hydrophobic and hydrophilic contact area. This analysis is limited in that bound water molecules were not considered in the crystal contact interactions since the criteria for modeling water molecules may vary among crystallographers and are also dependent on data quality. Several interactions could however involve hydrogen bonds to water molecules. Side chains with missing atoms were rebuilt in order to use the surface with an atom composition representing the true surface for the property calculations. They were however rebuilt automatically and could potentially be in a wrong orientation.

Comparing the residue identity of the crystal contacts for the crystals presented in Table 2 shows that seven of the interface residues are common for all crystal forms

**Table 2: Properties of crystal packing contact surfaces of insulin hexamers in seven different space groups.**

Protein	C2urea	C2scn	C222 <sub>1</sub> urea	C222 <sub>1</sub> scn	IEVR [11]	IEV3 [11]	MSO [9]	ITRZ [17]	nph-ins <sup>c</sup>
<b>Space group</b>	<b>C2</b>	<b>C2</b>	<b>C222<sub>1</sub></b>	<b>C222<sub>1</sub></b>	<b>P2<sub>1</sub></b>	<b>R3</b>	<b>R3</b>	<b>R3</b>	<b>P4<sub>3</sub>2<sub>1</sub>2</b>
<b>B-chain configuration</b>	R <sub>6</sub>	R <sub>6</sub>	R <sub>6</sub>	R <sub>6</sub>	R <sub>6</sub>	R <sub>6</sub>	T <sub>6</sub>	T <sub>3</sub> R <sub>3</sub> <sup>f</sup>	R <sub>6</sub>
<b>pH</b>	7.0	7.0	6.5	6.5	6.7	8.5	6.3	6.4	7.3
<b>Solvent content. (%)</b>	50	50	64	64	49	40	36		48
<b>Avg B-factor</b>									
<b>protein atoms (Å<sup>2</sup>)</b>	25.5	19.5	32.1	33.5	41.1	30.2	12.0	32.8	34.8
<b>exposed atoms (Å<sup>2</sup>)</b>	27.9	21.5	34.0	35.9	42.5	34	12.3	34.7	36.5
<b>contact atoms (Å<sup>2</sup>)</b>	25.0	17.6	26.4	29.1	41.9	35.8	14.1	37.2	34.3
<b>Tot SASA (Å<sup>2</sup>)<sup>a</sup></b>	14546	14478	40059	41532	15245	13573	13689	13904	15067
<b>A<sub>cont</sub>(Å<sup>2</sup>)<sup>b</sup></b>	2117	2226	4269	4060	2113	2006	3313	2438	2279
<b>fract of tot SASA (%)</b>	14.6	15.4	10.6	9.8	13.9	14.8	24.2	17.5	15.1
<b>Atom type specific area as a fraction of A<sub>cont</sub></b>									
<b>C area (%)</b>	55	56	53	53	41	45	46	50	48
<b>O area (%)</b>	25	24	31	32	33	35	37	32	38
<b>N area (%)</b>	21	20	16	15	27	20	18	16	14
<b>S area (%)</b>	0	0	0	0	0	0	0	2	0
<b>C aromatic (%)</b>	31	36	35	35	25	32	14	29	30
<b>C aliphatic (%)</b>	23	20	18	18	16	13	32	21	18
<b>Pos charged Area (%)</b>	5	3	3	3	5	0	16	16	2
<b>Neg charged Area (%)</b>	7	6	13	13	4	5	9	4	9

<sup>a</sup>SASA = Solvent accessible surface area.

<sup>b</sup>A<sub>cont</sub> = contact area between reference molecule and a symmetry related molecule.

<sup>c</sup>In house structure of human insulin co-crystallized with protamine.

(GlnA5, ThrA8, TyrA14, GlnA15, AsnA18, TyrA19 and PheB1). Altogether, the contact sites for the six crystal types compared in this study cover almost the entire surface of an insulin hexamer. A comparison of the exposed residues with the residues involved in crystal contacts shows that all residues with an exposure of more than 20% participate in some contact interface. The degree of exposure was calculated according to [25]. A number of studies, where crystal packing contacts have been systematically investigated [26,27] conclude that atomic composition within crystal contacts is indistinguishable from that of the protein surface and is rather non-specific. Studies of pancreatic ribonuclease [28] and cutinase [29], crystallized in a number of space groups, showed in accordance with the present study that virtually the entire protein surface can be involved in crystal contacts.

### Urea binding

The C222<sub>1</sub>urea and C2urea crystals were grown in presence of 3 M and 4 M urea, respectively. Seven urea molecules were built into the C2 structure. Five of these were located at equivalent positions in the monomers, Figure 6. The nitrogen atoms hydrogen bond primarily to the carbonyl oxygen of GlnA5, but the carbonyl oxygen of SerA9 and IleA10 are also within a reasonable hydrogen bond-

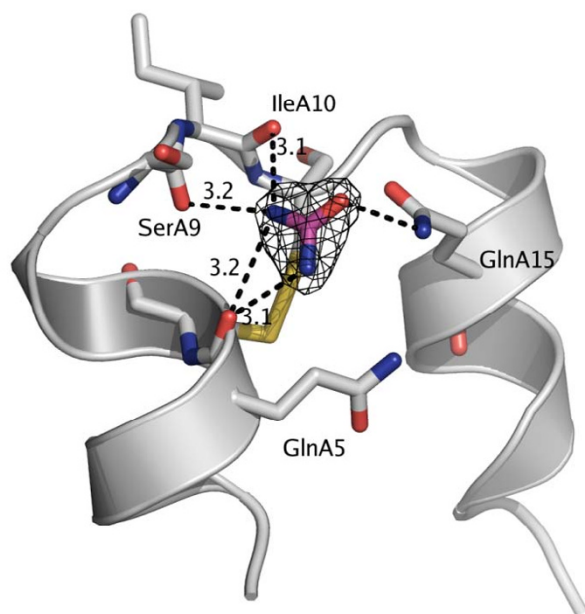


**Figure 6**  
**Urea binding site.** The most commonly occupied binding site for the urea molecule in the C2urea and C222<sub>1</sub>urea structures. Hydrogen bonds are primarily directed towards the carbonyl oxygen GlnA5 but surrounding carbonyl oxygens from SerA9 and IleA10 are within reasonable distances. Marked distances are given in Ångström (Å).

ing distance (average 3.1 Å). In monomer six, the urea is either disordered or not present. Instead, a water molecule was built into the density. Nine out of 18 possible equivalent positions in the C222<sub>1</sub> structure were occupied by urea. In the nine positions without a urea molecule, water was built in. Furthermore, these positions are more distant to a neighboring hexamer and therefore have a less well-defined electron density which may explain the inability to model a urea molecule. Exceptions from the above generalization are the monomers II.4 and III.1, which are close to a neighboring hexamer, but the electron density indicates two ordered water molecules.

Insulin has been shown to be tolerant of high concentrations of urea and other denaturants [30,31] and urea has previously been used to increase its solubility. One example is the inclusion of urea to promote growth of larger crystals of an insulin-protamine complex [32]. No significant conformational changes were detected in our structures as a result of direct urea interactions. In spite of its common use as a chemical denaturant of proteins, the molecular mechanism of urea-mediated unfolding is not known. Identification of denaturant interactions with proteins may give insight into the early stages of protein unfolding [33]. For a denaturant to be effective, protein-solvent interactions must be disturbed and this is thought to happen either through a direct or an indirect mechanism [34]. A direct mechanism would involve binding of urea molecules to the protein surface and thus compete with water-protein interactions and enhance the solubility of hydrophobic residues. Indirect urea denaturation would involve disruption of solvent-mediated hydrophobic interactions which would destabilize the protein structure. In addition, studies have shown that urea and guanidine hydrochloride at sub-denaturant concentrations stabilize proteins at a sub global level in a mechanism called protein stiffening [35,36]. The present study shows that urea at concentrations ~3 M has one specific binding site on the surface of the insulin molecule, interacting with backbone carbonyl groups of primarily GlnA5 but also of SerA9 and IleA10 residues. Given the high concentrations of urea present in the crystallization experiments, we would expect to detect even weak binding sites with a  $K_d$  of several hundred mM. Thus it seems unlikely that insulin denaturation occurs via a direct mechanism which requires binding of several urea molecules. On the other hand we see no signs of partial unfolding in our structures which would be indicative of an indirect mechanism. A recent study suggests that the denaturant effect of urea is neither due to a direct or indirect mechanism but rather an effect of a reduction of ion pairing between ionic and polar groups at aggregate surfaces [37], something which also could explain the relative higher fraction of non-polar surface at crystal contacts in our crystal forms.

## Conclusion

In spite of the extensive research on insulin crystallization during the last 80 years we could surprisingly identify two new crystal forms of human insulin. The major factor behind the change of space group from  $C222_1$  to  $C2$  was an increase in pH from  $\sim 6.5$  to 7.0. A comparison of the crystal contacts in the two space groups showed that the interfaces are very similar. The most obvious difference and the most remarkable contact interaction was the double TyrA14-TyrA14 interaction combined with a tight GluA17-GluA17 interaction. When taking all symmetry-related contacts into account it was found that this contact type was more frequent in the  $C222_1$  crystals when compared to the  $C2$  crystals. This crystal packing interaction has not been observed in any of the previously known insulin crystals. The addition of chaotropes such as urea and thiocyanate to the crystallization buffer can have an effect on the protein charge properties by charge screening. This could explain altered  $pK_a$  values of the glutamic acids involved in the crystal contacts and the higher fraction of hydrophobic crystal contacts in the present crystal forms compared to previously known insulin crystals. The short carboxyl-carboxyl interaction indicates the presence of a shared proton between the two groups and would be a strong low barrier hydrogen bond which should contribute to the stability of the crystals.

In the case of insulin, much effort has been put into the modification of the dimerization interactions [38,39] and hexamer formations [40,41], but less focus has been on the inter-hexamer interactions in solution or within crystals. Modifications of surface residues can induce changes in crystal packing due to breaking of existing interactions and/or formation of new ones [42,43]. Engineering of the protein surface to specifically induce a change in the crystal form or improve stability in lattice contacts may produce a better diffracting crystal [44]. Since insulin is a therapeutic protein administered also in crystalline form, the discovery and analysis of new polymorphic forms has implications beyond providing improved crystals for structural studies. The inter-hexamer interaction found in the present structures provides an interesting and novel interface that is specific for these two crystal forms. A single additional hydrophobic or several polar interactions may increase the half-life of a protein by several orders of magnitude [45]. Thus, additional inter-hexamer interactions can increase the stability and thus the shelf life of crystalline insulin formulations. The structures presented here provide a framework for further site-directed mutagenesis studies of the residues involved in inter-hexamer interactions, aimed at providing improved formulations useable within the rapidly advancing field of alternate delivery routes of crystalline biopharmaceuticals [3].

This study also demonstrates the usefulness of X-ray powder diffraction (XRPD) on protein samples. The small size of the initially obtained micro crystals made visual analysis and single crystal X-ray diffraction difficult. However, the combination of XRPD and principal component analysis (PCA) facilitated the identification of a new crystal form [21]. Since the use of proteins as therapeutic agents is a growing field, applications of protein XRPD, similar to the present study, will have an important role during discovery and development of therapeutic protein formulations.

## Methods

### Crystallization

Human insulin was obtained from Novo Nordisk A/S (Denmark). Crystals were grown by hanging-drop vapor diffusion technique at 291 K. The crystals were obtained in crystallization experiments with varying reservoir concentrations of NaCl and urea. A protein solution containing 6.9 mg/ml of human insulin, with zinc content corresponding to two zinc ions per hexamer and 50 mM resorcinol were mixed with equal volumes of reservoir solution. The protein solution was filtered through a 0.22-micrometer centrifugal filter (Ultrafree-MC, Millipore, USA) prior to crystallization. The best diffracting crystals were obtained from the following conditions. For the  $C222_1$  crystals: 2 M NaCl, 3 M urea, 100 mM phosphate buffer pH 6.5; for the  $C2$  crystals: 2.5 M NaCl, 4 M urea, 100 mM phosphate buffer pH 7.0. The same two crystal forms were obtained when including 15 mM NaSCN in the protein solution in absence of urea and using a reservoir solution containing 5% (v/v) ethanol and 200 mM phosphate buffer at pH 6.5 and 7.0, respectively. Crystals with dimensions of about 0.25 mm on one edge were detected after two days. The two orthorhombic crystals in space group  $C222_1$  diffracted to a resolution of 2.0 Å while data from the crystals in space group  $C2$  could be collected to 1.7 Å.

### Data collection and refinement

Data sets were collected from a single crystal of each type at 100 K using synchrotron radiation (Maxlab synchrotron, Lund, Sweden, beamline 911-2 and 911-3 [46]), with a MarMosaic 225 CCD detector (MarResearch, Evanston, USA). The urea containing crystals were soaked in a cryo-solution containing 23% glycerol and 77% reservoir prior to freezing in liquid nitrogen. For the NaSCN crystals a cryo-solution containing 30% glycerol was needed. All data sets were processed and scaled using the XDS package [47].

For the  $C222_1$  crystals with urea, an additional low-resolution data set was collected from the same crystal and merged with the high-resolution data. An in house structure of a hexamer with  $R_6$  conformation, excluding all

non-protein atoms except zinc, was used as search model for molecular replacement in Molrep [48]. Three hexamers were found in the asymmetric unit, corresponding to a solvent content of 64%. During refinement in Refmac [49], 5% of the data was excluded and used for calculation of the R-free value. The initial  $2F_o - F_c$  map clearly indicated positions of chloride ions and resorcinol molecules (six in each hexamer). After several rounds of refinement using the maximum likelihood option in Refmac and manual adjustments of main-chain and side-chain atoms in Coot [50], TLS refinement [51] was employed, with each monomer defined as a separate TLS group. Subsequently, water was added by the find-water function in Coot. At the end of the refinement, urea molecules were modeled into the electron density using positive  $F_o - F_c$  peaks, where the shape of the  $2F_o - F_c$  density was flat and reminiscent of the triangular shape of a urea molecule. 14 such positions were found with an average B-factor of  $53.1 \text{ \AA}^2$ . The final number of water molecules was 634 with an average B-factor of  $41.7 \text{ \AA}^2$ .

The C2 structure obtained with urea was solved with the same search model as the C222<sub>1</sub> data set and the procedure for structure solving and refinement followed the same route. In the beginning of the refinement, there was a clear  $2F_o - F_c$  density for an extra resorcinol binding site, and at later stages of refinement, a second additional position showed density resembling a resorcinol molecule. Seven urea molecules (average B-factor =  $39.3 \text{ \AA}^2$ ) and 257 water molecules were built into the density at the end of refinement.

For the two structures co-crystallized with NaSCN, one high and one low resolution data set were collected and subsequently merged. The structures were solved using the urea containing structures as search models in molecular replacement rounds (excluding non-protein atoms except zinc). Based on the experience of flexible residues in the B-chain terminals, the search models were truncated at both ends to reduce bias (PheB1, ValB2, LysB29 and ThrB30). Refinement followed the same scheme as for the urea crystals. In total, six resorcinol molecules were modeled into the C2 structure and 18 in the C222<sub>1</sub> structure (six in each hexamer). 313 water molecules were fitted into the C2 structure and 755 into the C222<sub>1</sub>. Based on the shape of the electron density, each zinc atom was found to interact with one thiocyanate molecule. Data collection details and refinement statistics for all four structures are summarized in Table 1. In this paper, the crystals obtained in presence of urea will be referred to as C222<sub>1</sub>urea and C2urea whilst the two forms obtained with thiocyanate are referred to as C222<sub>1</sub>scn and C2scn.

### Analysis of crystal packing

Symmetry-related molecules were generated in Pymol [52] for analysis of crystal contacts. A rather strict criterion for identification of symmetry contacts was used by searching for symmetry-related atoms within  $4 \text{ \AA}$  from the reference protein. In order to limit the analysis to protein-protein interactions, non-protein atoms such as water and urea molecules were removed prior to searches. Residues with missing side-chain atoms were reconstructed in Swiss-PdbViewer [53] using the 'auto reconstruct residues with missing atom' function. When dual conformations of residue side chains were present, the one with highest occupancy, or when equal, the conformation denoted with an 'A' in the pdb file was chosen. The contact area ( $A_{\text{cont}}$ ) between the reference molecule and neighboring symmetry-related molecules was defined as the solvent accessible area buried by symmetry-related molecules. The solvent accessible surface area (SASA) was calculated in areaMol (within the CCP4 program package [54]) that utilizes the algorithm of Lee & Richards [55]. A water probe of  $1.4 \text{ \AA}$  was used.  $A_{\text{cont}}$  for each atom was obtained by taking the SASA for the reference molecule alone, minus the SASA when contact atoms were present. All atoms with reduced SASA were assumed to be involved in contacts with a symmetry molecule. Basic physicochemical properties related to hydrophobic surface area were calculated for the atoms of the reference molecule involved in contacts. Contact areas were split into hydrophobic (carbons) and hydrophilic (nitrogen and oxygens), aliphatic-, aromatic carbons and positive-, negative charged area. For the sake of simplicity and ease of comparison, crystals without a full hexamer in the asymmetric unit were complemented with the required symmetry molecules by applying appropriate symmetry operations to generate a hexamer prior to calculations. A hexamer was considered as one molecule.

Coordinates with structure factors have been deposited to the Protein Data Bank (PDB) [56] with the accession codes [2OLY](#), [2OLZ](#), [2OM0](#) and [2OM1](#).

### Authors' contributions

MN collected and interpreted the data and drafted the manuscript. GS conceived the study and participated in the crystallization experiments and interpretation of results. Both authors read and approved the final version of the manuscript.

### Acknowledgements

We thank Lene Drube and Berit Bergerud Hansen for technical assistance and Salam Al-Karadaghi and Eva Johansson for valuable input during the preparation of this manuscript. The work was supported by the VTU (Ministry of Science, Technology and Innovation), Denmark and the Novo Nordisk CORA Training and research program.

## References

1. Banting FG, Best CH: **Insulin its chemistry and physiology.** *J Lab Clin Med* 1922, **7**:251-266.
2. Adams MJ, Blundell TL, Dodson EJ, Dodson GG, Vijayan M, Baker EN, Harding MM, Hodgkin DC, Rimmer B, Sheat S: **Structure of Rhombohedral 2 Zinc Insulin Crystals.** *Nature* 1969, **224**:491-495.
3. Basu SK, Govardhan CP, Jung CW, Margolin AL: **Protein crystals for the delivery of biopharmaceuticals.** *Expert Opin Biol Ther* 2004, **4**:301-317.
4. DeFelippis MR, Dobbins MA: **Insulin crystals for pulmonary administration.** In *Patent Eli Lilly*; 2001:PCT/US00/15026.
5. Havelund S: **Zinc free insulin crystals for use in pulmonary compositions.** In *Patent Novo Nordisk A/S*; 1998:PCT/DK98/00109.
6. Schlichtkrull J: **Chemical and biological studies on insulin crystals and insulin zinc suspensions.** In *Thesis University of Copenhagen*; 1958.
7. Kaarsholm NC, Ko HC, Dunn MF: **Comparison of Solution Structural Flexibility and Zinc Binding Domains for Insulin, Proinsulin, and Miniproinsulin.** *Biochemistry* 1989, **28**:4427-4435.
8. Baker EN, Blundell TL, Cutfield JF, Cutfield SM, Dodson EJ, Dodson GG, Hodgkin DM, Hubbard RE, Isaacs NW, Reynolds CD: **The structure of 2Zn pig insulin crystals at 1.5 Å resolution.** *Philos Trans R Soc London Ser B* 1988, **319**:369-456.
9. Smith GD, Pangborn WA, Blessing RH: **The structure of T6 human insulin at 1.0 Å resolution.** *Acta Crystallogr D Biol Crystallogr* 2003, **59**(Pt 3):474-482.
10. Derewenda U, Derewenda Z, Dodson EJ, Dodson GG, Reynolds CD, Smith GD, Sparks C, Swenson D: **Phenol stabilizes more helix in a new symmetrical zinc insulin hexamer.** *Nature* 1989, **338**:594-596.
11. Smith GD, Ciszak E, Magrum LA, Pangborn WA, Blessing RH: **R6 hexameric insulin complexed with m-cresol or resorcinol.** *Acta Crystallogr D Biol Crystallogr* 2000, **56**(Pt 12):1541-1548.
12. Smith GD, Dodson GG: **Structure of a rhombohedral R6 insulin/phenol complex.** *Proteins* 1992, **14**:401-408.
13. Whittingham JL, Edwards DJ, Antson AA, Clarkson JM, Dodson GG: **Interactions of Phenol and m-Cresol in the Insulin Hexamer, and Their Effect on the Association Properties of B28 Pro Asp Insulin Analogues.** *Biochemistry* 1998, **37**:11516-11523.
14. Roy M, Brader ML, Lee RW, Kaarsholm NC, Hansen JF, Dunn MF: **Spectroscopic signatures of the T to R conformational transition in the insulin hexamer.** *J Biol Chem* 1989, **264**:19081-19085.
15. Brader ML, Dunn MF: **Insulin hexamers: new conformations and applications.** *Trends Biochem Sci* 1991, **16**:341-345.
16. Whittingham JL, Chaudhuri S, Dodson EJ, Moody PCE, Dodson G: **X-ray Crystallographic Studies on Hexameric Insulins in the Presence of Helix-S stabilizing Agents, Thiocyanate, Methylparaben, and Phenol.** *Biochemistry* 1995, **34**:15553-15563.
17. Ciszak E, Smith GD: **Crystallographic evidence for dual coordination around zinc in the T3R3 human insulin hexamer.** *Biochemistry* 1994, **33**:1512-1517.
18. Abel JJ: **Crystalline Insulin.** *Proc Natl Acad Sci U S A* 1926, **12**:132-136.
19. Scott DA: **Crystalline insulin.** *Biochem J* 1934, **28**:1592-151602.
20. Krayenbuhl C, Rosenberg T: **Crystalline protamine insulin.** *Rep Steno Mem Hosp Nord Insulinlab* 1946, **1**:60-73.
21. Norrman M, Stahl K, Schluckebier G, Al Karadaghi S: **Characterization of insulin microcrystals using powder diffraction and multivariate data analysis.** *J Appl Cryst* 2006, **39**:391-400.
22. Cleland WW, Frey PA, Gerlt JA: **The Low Barrier Hydrogen Bond in Enzymatic Catalysis.** *J Biol Chem* 1998, **273**:25529-25532.
23. Wohlfahrt G: **Analysis of pH-dependent elements in proteins: Geometry and properties of pairs of hydrogen-bonded carboxylic acid side-chains.** *Proteins: Structure, Function, and Bioinformatics* 2005, **58**:396-406.
24. Flocco MM, Mowbray SL: **Strange Bedfellows: Interactions between Acidic Side-chains in Proteins.** *J Mol Biol* 1995, **254**:96-105.
25. Miller S, Janin J, Lesk AM, Chothia C: **Interior and surface of monomeric proteins.** *J Mol Biol* 1987, **196**:641-656.
26. Carugo O, Argos P: **Protein-protein crystal-packing contacts.** *Protein Sci* 1997, **6**:2261-2263.
27. Janin J, Rodier F: **Protein-protein interaction at crystal contacts.** *Proteins* 1995, **23**:580-587.
28. Crosio MP, Janin J, Jullien M: **Crystal packing in six crystal forms of pancreatic ribonuclease.** *J Mol Biol* 1992, **228**:243-251.
29. Jelsch C, Longhi S, Cambillau C: **Packing forces in nine crystal forms of cutinase.** *Proteins: Structure, Function and Genetics* 1998, **31**:320-333.
30. Bryant C, Strohl M, Green LK, Long HB, Alter LA, Pekar AH, Chance RE, Brems DN: **Detection of an equilibrium intermediate in the folding of a monomeric insulin analog.** *Biochemistry* 1992, **31**:5692-5698.
31. Brems DN, Brown PL, Heckenlaible LA, Frank BH: **Equilibrium denaturation of insulin and proinsulin.** *Biochemistry* 1990, **29**:9289-9293.
32. Balschmidt P, Hansen FB, Dodson EJ, Dodson GG, Korber F: **Structure of porcine insulin cocrystallized with clupeine Z.** *Acta Crystallogr B* 1991, **47**(Pt 6):975-986.
33. Dobson CM, Evans PA, Radford SE: **Understanding how proteins fold: the lysozyme story so far.** *Trends Biochem Sci* 1994, **19**:31-37.
34. Robinson DR, Jencks WP: **The effect of compounds of the urea-guanidinium class on the activity coefficient of acetyltetraglycine ethyl ester and related compounds.** *J Am Chem Soc* 1965, **87**:2462-2470.
35. Bhuyan AK: **Protein Stabilization by Urea and Guanidine Hydrochloride.** *Biochemistry* 2002, **41**:13386-13394.
36. Kumar R, Prabhu NP, Yadaiah M, Bhuyan AK: **Protein Stiffening and Entropic Stabilization in the Subdenaturing Limit of Guanidine Hydrochloride.** *Biophys J* 2004, **87**:2656-2662.
37. Dias LG, Florenzano FH, Reed WF, Baptista MS, Souza SMB, Alvarez EB, Chaimovich H, Cuccovia IM, Amaral CLC, Brasil CR, Rostmed LS, Politi MJ: **Effect of Urea on Biomimetic Systems: Neither Water 3-D Structure Rupture nor Direct Mechanism, Simply a More "Polar Water".** *Langmuir* 2002, **18**:319-324.
38. Brange J: **The new era of biotech insulin analogues.** *Diabetologia* 1997, **40** Suppl 2:S48-S53.
39. Brange J, Ribel U, Hansen JF, Dodson G, Hansen MT, Havelund S, Melberg SG, Norris F, Norris K, Snel L, Sørensen AR, Voigt HO: **Monomeric insulins obtained by protein engineering and their medical implications.** *Nature* 1988, **333**:679-682.
40. Bentley GA, Brange J, Derewenda Z, Dodson EJ, Dodson GG, Markussen J, Wilkinson AJ, Wollmer A, Xiao B: **Role of B13 glu in insulin assembly - the hexamer structure of recombinant mutant (B13 glu->gln) insulin.** *J Mol Biol* 1992, **228**:1163-1176.
41. Vajo Z, Duckworth WC: **Genetically Engineered Insulin Analogs: Diabetes in the New Millennium.** *Pharmacol Rev* 2000, **52**:1-10.
42. D'Arcy A, Stihle M, Kostrewa D, Dale G: **Crystal engineering: a case study using the 24 kDa fragment of the DNA gyrase B subunit from Escherichia coli.** *Acta Crystallogr D Biol Crystallogr* 1999, **55**(Pt 9):1623-1625.
43. Xiao B, Dodson GG, Dodson EJ, Clarkson J, Turkenburg J, Derewenda U, Brady L, Brange J: **Mutant insulin crystal packing.** *J Cryst Growth* 1992, **122**:144-151.
44. Derewenda ZS, Vekilov PG: **Entropy and surface engineering in protein crystallization.** *Acta Crystallogr D Biol Crystallogr* 2006, **62**(Pt 1):116-124.
45. Daniel RM: **The upper limits of enzyme thermal stability.** *Enzyme Microb Technol* 1996, **19**:74-79.
46. Mammen CB, Ursby T, Cerenius Y, Thunnissen M, Als-Nielsen J, Larsen S, Liljas A: **Design of a 5-Station Macromolecular Crystallography Beamline at MAX-Lab.** *Acta Physica Polonica A* 2002, **101**:595-602.
47. Kabsch W: **Automatic processing of rotation diffraction data from crystals of initially unknown symmetry and cell constants.** *J Appl Cryst* 1993, **26**:795-800.
48. Vagin A, Teplyakov A: **MOLREP: an Automated Program for Molecular Replacement.** *J Appl Cryst* 1997, **30**:1022-1025.
49. Murshudov GN, Vagin AA, Dodson EJ: **Refinement of macromolecular structures by the maximum-likelihood method.** *Acta Crystallogr D Biol Crystallogr* 1997, **53**(Pt 3):240-255.
50. Emsley P, Cowtan K: **Coot: model-building tools for molecular graphics.** *Acta Crystallogr D Biol Crystallogr* 2004, **60**(Pt 12 Pt 1):2126-2132.
51. Winn MD, Isupov MN, Murshudov GN: **Use of TLS parameters to model anisotropic displacements in macromolecular**

- refinement.** *Acta Crystallogr D Biol Crystallogr* 2001, **57(Pt 1)**:122-133.
52. DeLano WL: **The PyMOL Molecular Graphics System.** San Carlos, CA, USA, DeLano Scientific; 2002.
53. Guex N, Peitsch MC: **SWISS-MODEL and the Swiss-Pdb-Viewer: an environment for comparative protein modeling.** *Electrophoresis* 1997, **18**:2714-2723.
54. Collaborative Computational Project, Number 4: **The CCP4 suite: programs for protein crystallography.** *Acta Crystallogr D Biol Crystallogr* 1994, **50(Pt 5)**:760-763.
55. Lee B, Richards FM: **The interpretation of protein structures: estimation of static accessibility.** *J Mol Biol* 1971, **55**:379-400.
56. Berman HM, Westbrook J, Feng Z, Gilliland G, Bhat TN, Weissig H, Shindyalov IN, Bourne PE: **The Protein Data Bank.** *Nucl Acids Res* 2000, **28**:235-242.

Publish with **BioMed Central** and every scientist can read your work free of charge

*"BioMed Central will be the most significant development for disseminating the results of biomedical research in our lifetime."*

Sir Paul Nurse, Cancer Research UK

Your research papers will be:

- available free of charge to the entire biomedical community
- peer reviewed and published immediately upon acceptance
- cited in PubMed and archived on PubMed Central
- yours — you keep the copyright

Submit your manuscript here:  
[http://www.biomedcentral.com/info/publishing\\_adv.asp](http://www.biomedcentral.com/info/publishing_adv.asp)

